International Conference on Space Optics—ICSO 2012

Ajaccio, Corse

9–12 October 2012

Edited by Bruno Cugny, Errico Armandillo, and Nikos Karafolas

Conception and test of echoes, a spectro-imager dedicated to the seismology of Jupiter

L. Soulat

F.-X. Schmider

S. Robbe-Dubois

T. Appourchaux

et al.

International Conference on Space Optics — ICSO 2012, edited by Bruno Cugny, Errico Armandillo, Nikos Karafolas
Proc. of SPIE Vol. 10564, 105641V · © 2012 ESA and CNES · CCC code: 0277-786X/17/$18 · doi: 10.1117/12.2309197

Conception and test of *Echoes*, a spectro-imager dedicated to the seismology of Jupiter

L. Soulat[1*], F.-X. Schmider[1], S. Robbe-Dubois[1], T. Appourchaux[2], P. Gaulme[3], Y. Bresson[1], J. Gay[1], J.-B. Daban[1], C. Gouvret[1]

[1]Laboratoire Lagrange, UMR 7293, Université de Nice Sophia-Antipolis, CNRS, Observatoire de la Côte d'Azur, 06300 Nice, France
[2]Institut d'Astrophysique Spatiale, Université Paris XI, UMR 8617, 91405 Orsay Cedex, France
[3]New Mexico State University, Department of Astronomy, Las Cruces, NM 88001, USA
laurence.soulat@unice.fr

ABSTRACT

Echoes is a project of a spaceborne Doppler Spectro-Imager (DSI) which has been proposed as payload to the JUICE mission project selected in the Cosmic Vision program of the European Space Agency (ESA). It is a Fourier transform spectrometer which measures phase shifts in the interference patterns induced by Doppler shifts of spectral lines reflected at the surface of the planet. Dedicated to the seismology of Jupiter, the instrument is designed to analyze the periodic movements induced by internal acoustic modes of the planet. It will allow the knowledge of the internal structure of Jupiter, in particular of the central region, which is essential for the comprehension of the scenario of the giant planets' formation. The optical design is based on a modified Mach-Zehnder interferometer operating in the visible domain and takes carefully into account the sensitivity of the optical path difference to the temperature. The instrument produces simultaneously four images in quadrature which allows the measurement of the phase without being contaminated by the continuum component of the incident light. We expect a noise level less than 1 $cm^2s^{-2}\mu Hz^{-1}$ in the frequency range [0.5 -10] mHz. In this paper, we present the prototype implemented at the Observatoire de la Côte d'Azur (OCA) in collaboration with Institut d'Astrophysique Spatiale (IAS) to study the real performances in laboratory and to demonstrate the capability to reach the required Technology Readiness Level 5.

Keywords: Fourier transform spectrometry – Seismology – Jupiter interior – Cosmic Vision

I. INTRODUCTION

Observations of Jupiter oscillations have been performed with several techniques. Deming et al. observed in the thermal infrared (1989), Schmider et al. used Doppler spectrometry with a sodium cell (1991) and Mosser et al. tried the Fourier transform spectrometry (1993 & 2000). These observations were limited by the fast rotation of the planet leading to results incompatible with theory. To overcome the limitations, Schmider et al. (2007) and Gaulme et al. (2008) proposed to achieve multi-sites observations with an instrument based on a Mach-Zehnder interferometer, called SYMPA (Seismic Imaging Interferometer for Monitoring Planetary Atmospheres). Three campaigns of observations have been carried out with two instruments, one by site, between 2003 and 2005. The recent data analysis (Gaulme et al. 2011) put in evidence the detection of Jovian pulsations conform to the theoretical models. Nevertheless, the identification of the modes on a spherical harmonic basis was unfortunately impossible, because of the low duty cycle and of the atmospheric turbulence. This is the reason why we propose to achieve the observations from space, with a space-borne instrument.

In this paper, we present the prototype of the Doppler Spectro-Imager *Echoes* [8]. The instrument principle is directly inherited from SYMPA. The study, funded by the Centre National d'Etudes Spatiales (CNES), is focused on the Mach-Zehnder interferometer. The first paragraph details the optical design of the Mach-Zehnder and the theoretical performances. The second paragraph explains the measurements to be achieved thanks to a dedicated test bench. Finally, the last paragraph presents the first experimental results obtained on the prototype.

II. OPTICAL DESIGN

A. Design description

The instrumental concept is studied to form four images in phase quadrature. The Mach-Zehnder (MZ) interferometer is placed in a parallel beam. The four outputs of the MZ are folded on a single detector by the four corner mirrors (M1, M2, M3, M4) and form four images thanks to four identical objectives. From these four images, we can use the "ABCD" method (Wyant 1975) which permits to get rid of the continuum component of the incident light. These images are obtained thanks to a specific optical design, based on a modified MZ interferometer (Fig. 1).
The "empty MZ" is composed of two blocks (K1 and K2) made in K5G20. These blocks are composed of two optical elements glued together and separated by a semi reflective treatment. Because the size of these blocks is different, an "empty" Optical Path Difference (OPD) is introduced.

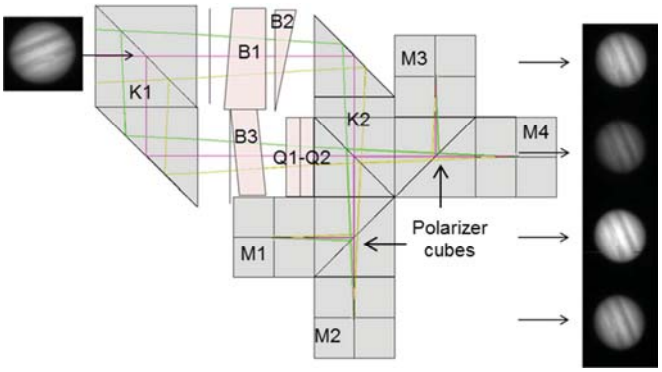

Figure 1: Optical design of the Mach-Zehnder

The sensitivity of the MZ to velocity field is the result of an optimization increasing the sensitivity of the phase and decreasing the contrast with the OPD change. By exploration of the solar spectrum, we looked for features giving contrast maxima. The best sensitivity is obtained for an OPD of 5048 µm at 519.5 nm. This OPD is created by introducing glass plates in the arms of the interferometer. A tilted plate in BK7G18 is placed in each arm in order to eliminate stray light and to make the fringes regular and rectilinear (B1-B2 and B3). One of the plates is sliced into two parts, the prismatic one (B2) being mounted on a piezoelectric plate in order to achieve the OPD modulation. The modulation will be helpful to blur the fringes during the pixel sensitivity calibration processes, but its main function is to create phase shifts of kπ/2 (k = 0, 1, 2, 3) to calibrate the response of each channel. Finally, a quarter wave plate, based on two quartz plates with perpendicular optical axes (Q1 and Q2), achieves the phase quadrature. Then, polarizer cubes are placed at each output and produce a kπ/2 phase shift. So we obtain four images in phase quadrature:

$$I_1 = \frac{I_0}{4}\{1 + \gamma \cos\phi\} \quad (1)$$

$$I_2 = \frac{I_0}{4}\{1 + \gamma \sin\phi\} \quad (2)$$

$$I_3 = \frac{I_0}{4}\{1 - \gamma \cos\phi\} \quad (3)$$

$$I_4 = \frac{I_0}{4}\{1 - \gamma \sin\phi\} \quad (4)$$

Where I_0 is the continuum component of the incident light, γ is the fringe contrast and ϕ is the fringe phase that we want to measure. From the phase measurement, we can obtain the radial velocity v_r which contains the information:

$$v_r = \frac{\phi \lambda_0 c}{2\pi\Delta} \quad (5)$$

where λ_0 is the central wavelength, Δ the OPD and c the speed of light.

The choice of the optical glasses respects two criteria. First, materials must be resistant to radiations. Then, thermal dilatation coefficients must compensate refractive index variations. That is why we have selected: K5G20 and BK7G18 from Schott, and crystalline quartz wave plates.

B. Optimization of the thermal stability

In order to ensure the best thermal stability, the MZ must operate at a precise temperature, called stability temperature. Simulations of the phase versus temperature result in a minimization of the thermal effect for a value of the temperature of 18.9°C. If the experimental temperature does not respect this condition, the optical parameters of the MZ have to be redefined. Indeed, there is a relation between glass plate thicknesses and stability temperature.

The protocol consists in measuring the phase of the fringes at different temperatures (5 measurement points are sufficient). The Figure 2 represents the theoretical phase in function of the temperature, and the fit of this curve.

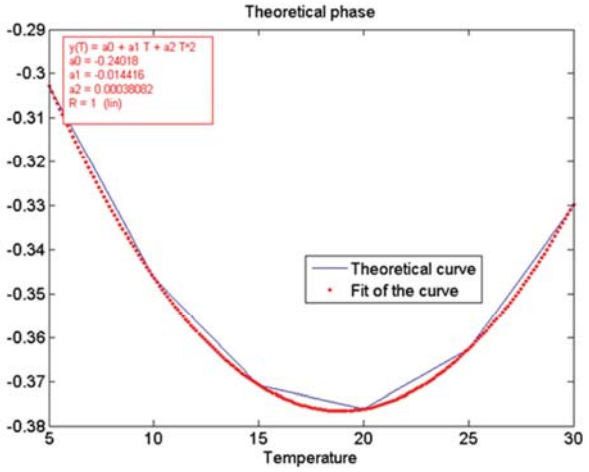

Figure 2: Fringe phase versus temperature

From the equation of the fit curve, we can deduce the stability temperature which is located at the minimum of the curve. The image processing allows the stability temperature determination with a precision of 0.01°C. A modification of the plate thickness will lead in a change in this stability temperature. An interesting point is that the BK7G18 plates have an effect on the stability temperature and on the OPD whereas the quartz plates only impact the OPD. The protocol will consist in adjusting the stability temperature T_s to the required value by modifying the thicknesses of the BK7G18 plates e_B. Then, the OPD will be retrieved by the adapted modification on the quartz plate thickness e_Q.

$$e_B + 12\ \mu m \rightarrow T_s + 1°C \rightarrow OPD + 6{,}3\ \mu m \quad (6)$$

$$e_Q - 12\ \mu m \rightarrow T_s - 0.01°C \rightarrow OPD - 6{,}6\ \mu m \quad (7)$$

As the thicknesses will be modified, the first version of the prototype will not be glued. The optical elements will be maintained mechanically or by molecular adherence.

C. *Theoretical performances*

The aim of *Echoes* is to analyze the solar spectral lines reflected at the surface of Jupiter. That is why it must operate in the visible domain. On top of that, the quantum efficiency of the detectors is better in the visible. Considering this requirement, the maximum of sensitivity is reached with the optimized parameters given in Table 1:

Table 1: Theoretical performances

OPD	5048 µm
Central Wavelength (λ_0)	519.5 nm
Filter band pass (FWHM)	1 nm
Field of View (FoV)	± 2.9°

Considering these performances, the theoretical fringe contrast is 5%. The FoV is determined to observe the whole planet at a minimal distance of 0.02 AU. It corresponds to an input pupil size of 2 cm.

III. EXPERIMENTAL STUDY OF THE PROTOTYPE

In this paragraph, we present the tests and controls to be achieved on the prototype with respect to the specifications listed in Table 2.

Table 2: Specifications to be respected

Name	Specification
Differential transmission	< 5%
Wavefront quality	26 nm rms (λ/20 @ 519.5 nm)
Phase quadrature	90° ± 10°
OPD	5048 µm ± 10 µm
Fringe contrast	5%
Loss of contrast	< 5% of the theoretical contrast
Stability temperature	18.9°C ± 0.1°C
Variation of the thermal sensitivity of the OPD	< 20 m s^{-1} K^{-1} in the FoV
Parallelism of output beams	< 20''

In order to verify the specifications, a dedicated test bench is implemented (Fig. 3).
The light source is provided by an integrating sphere. The MZ will be integrated in a thermal vacuum tank. A combination of polarizer cubes and mirrors, called "Periscope - Polarizer", separates the image in two: one by polarization direction. The desired wavelength is observed in the seventh order. Finally, two images are observed side by side on the detector.

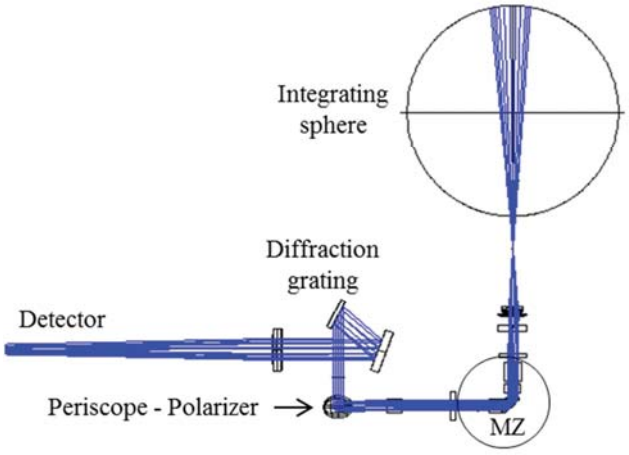

Figure 3: Optical test bench

The tests and controls to be achieved on the prototype are divided into three main parts:

- Calibration and alignment of the test bench (calibration of the diffraction grating dispersion, polarization of the optical elements).
- Control of the Mach-Zehnder (transmission, polarization and wavefront quality in each arm, parallelism of the output beams, phase shift between the two arms).
- Adjustment of the Mach-Zehnder (adjustment of the OPD, maximization of the contrast, determination of the stability temperature).

A software developed at OCA permits the control of the test bench and the acquisition of the images. We can adjust the parameters of the detector (image size, gain, etc.), the temperature of the cooler and the position of the piezoelectric plate. Matlab programs are included in the software for the image processing: determination of the OPD, of the fringe contrast and of the stability temperature. With this interface, we can adjust the Mach-Zehnder while viewing the result in real time. The image processing allows reaching the required precisions to respect the specifications.

IV. CONTROL OF THE SEMI REFLECTIVE COATINGS

In this paragraph, we present the first results obtained on the K1 and K2 blocks (Fig 1). The aim is to control the semi reflective coatings before the integration of the Mach-Zehnder to verify if the specifications on the transmission and on the phase quadrature are respected.
The semi-reflective coatings are specified to transmit and reflect 50% of the incident light regardless of the polarization. The absorption must be less than 3%.

A. *Control of the transmissions*

A first test bench for the control of the transmission of the blocks has been implemented (Fig. 4). This bench consists in measuring the photometry at the two outputs of each prism.

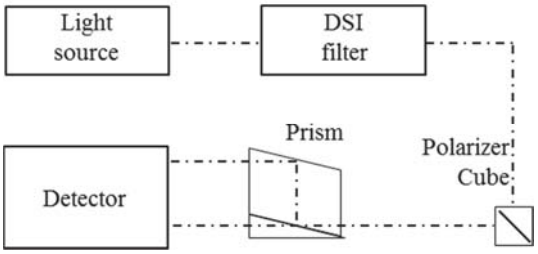

Figure 4: Test bench for the transmission control

We occult one path and we acquire series of images. We repeat the process for the other arm. Measurements have been achieved separately on each prism block. The values of transmissions and reflections are measured in each polarization, P and S, and are given in Table 3.

Table 3: Measured transmissions and reflections of the coatings

	$T_{\parallel}$	$R_{\parallel}$	$T_{\perp}$	$R_{\perp}$
K1 block	0.56	0.35	0.56	0.35
K2 block	0.56	0.35	0.52	0.36

From these values, we can determine the transmission and the contrast at each output of the Mach-Zehnder, for each polarization (Table 4).

Table 4: Transmission and contrast at each output

	Transmission	Contrast
Output_1	$\sqrt{R1_{\parallel}T2_{\parallel}} + \sqrt{T1_{\parallel}R2_{\parallel}} = 0.885$	0.885
Output_2	$\sqrt{R1_{\parallel}R2_{\parallel}} + \sqrt{T1_{\parallel}T2_{\parallel}} = 0.910$	0.862
Output_3	$\sqrt{R1_{\perp}T2_{\perp}} + \sqrt{T1_{\perp}R2_{\perp}} = 0.876$	0.875
Output_4	$\sqrt{R1_{\perp}R2_{\perp}} + \sqrt{T1_{\perp}T2_{\perp}} = 0.895$	0.856

We can see that the differential transmission is less than 2% which respects the specification of 5%. The absorption of the coatings is around 12% which does not respect the specification of 3%. Section (4.3.) gives the consequence of these measured values on the expected performance.

B. Control of the polarization

The dedicated test bench (see section 3.) is now used to control the polarization of the coatings. A light source is injected through an adjustable slit and directed to the MZ. A combination of mirrors is studied to image easily each output separately. At the output of the MZ, we have the "periscope – polarizer" module, the diffraction grating and finally, the interferential filter which is placed upstream of the detector (Fig. 5).

The Fig. 6 represents parts of the images obtained at each output of the MZ, resized for the image processing.

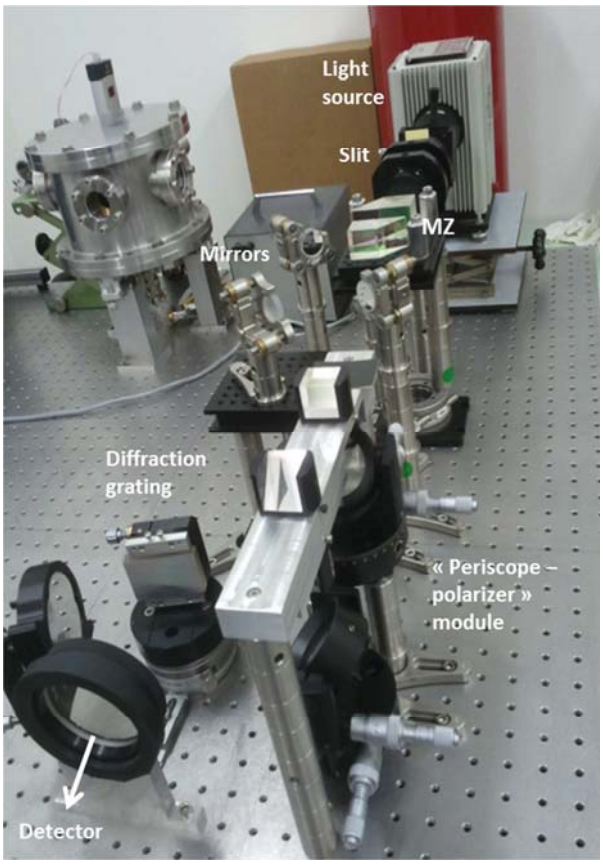

Figure 5: Test bench for the phase shift control

The "empty MZ" produces interference fringes because the size of the two blocks K1 and K2 is different. Fringes are obtained in the spectral and spatial dimensions (the OPD varies with the wavelength and with the FoV).

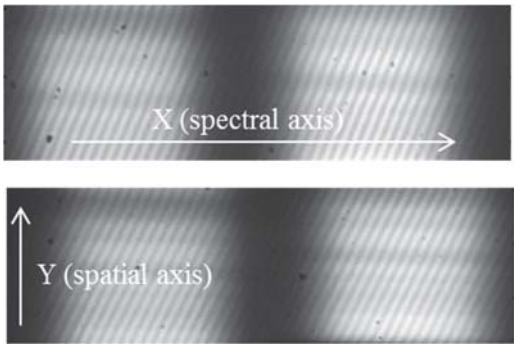

Figure 6: Images obtained at each output of the MZ

Protocol of the phase shift calculation:

- Determination of a Y_0 reference position in Y, calculated by cross-correlation
- Determination of the filter profile in X at this position Y_0 for spectral calibration
- Determination of the position X_0 of the filter maximum of transmission by a fit

- Calculation of the phase at this position (X_0,Y_0) for each output and each polarization. The phase is given by the argument of the Fourier transform.
- Calculation of the phase shift for each polarization

The theoretical phase shift between the two outputs of the MZ is 180°. The error to the phase quadrature is $\Delta\Phi_1$ in the polarization 1 and $\Delta\Phi_2$ in the polarization 2. The results (averages over several images) are the following:

$$\Delta\Phi_1 = 10.44° \quad \text{and} \quad \Delta\Phi_2 = 10.61°$$

These results give an idea of the precision of the measurement, of the order of a few degrees, sufficient for our task. The specification of the error to the phase quadrature is reached. We notice that the difference between the two polarizations is low, so it will not increase the noise level in the phase measurement. These preliminary results will be supplemented by other measurements.

C. Acceptance

The standard deviation on the velocity variations due to the photon noise is given by:

$$\delta_v = \frac{c}{2\pi\sigma_0\gamma\sqrt{2N}} \tag{8}$$

where σ_0 is the central wavenumber and N the total number of photons. By considering the measured transmissions (4.1.) and the errors to the phase quadrature (4.2.), the degradation of the performances in terms of velocity measurement is 23% (Eq. 8).

The study being limited to a R&D, we decided to accept the coatings with present values, although slightly out the specification range, in order to achieve the complete test set. Indeed, the most crucial part of the test is the thermal sensitivity and the final adjustment of the MZ, and the determination of the calibration procedure.

V. CONCLUSION AND PERSPECTIVE

As the first results have been achieved and accepted, the prototype is currently under integration. The test bench has been implemented, and the calibration of the diffraction grating will occur in September 2012. As this calibration requires working with the solar light, optical fibers will achieve the light path from outdoor to the test bench.

The control of the Mach-Zehnder will be finished this autumn: differential transmission, wavefront quality, parallelism of the output beams and phase shift between the two outputs. We expect the adjustment for the end of 2012: adjustment of the OPD, maximization of the contrast and determination of the stability temperature. When the thicknesses will be modified (cf. section 2.2.), we will achieve the measurement of the thermal stability which requires the detection of an OPD variation of 170 pm. The Mach-Zehnder will be integrated in a thermal vacuum tank regulated at ± 0.4° by a cooler.

We plan an adaptation of the prototype to be placed on the MEO telescope (Calern, France) to achieve observations of Jupiter at the end of 2013. It is important to validate the performances of the instrument in real observation conditions.

ACKNOWLEDGMENT

The authors are very grateful to the Centre National d'Etudes Spatiales (CNES) and Thales Alenia Space (TAS) for the thesis funding, and CNES for the support for the Mach-Zehnder R&D.

REFERENCES

[1] Deming, D., Mumma, M. J., Espenak, F., et al, ApJ, 343, 456 (1989).
[2] Gaulme, P.; Schmider, F. -X., et al., SYMPA, a dedicated instrument for Jovian seismology. II. Real performance and first results, *Astronomy and Astrophysics*, Volume 490, Issue 2, pp.859-871 (2008).
[3] Gaulme, P.; Schmider F.-X.; Gay, J.; Guillot, T.; Jacob, C.; Detection of Jovian seismic waves: a new probe of its interior structure, *Astronomy & Astrophysics*, Volume 531, id.A104 (2011).
[4] Mosser, B., Mekarnia, D., Maillard, J.-P., et al, *Astronomy & Astrophysics*, 267, 604 (1993).
[5] Mosser, B., Maillard, J. P., & Mékarnia, D., Icarus, 144, 104 (2000).
[6] Schmider, F.-X., Fossat, E., & Mosser, B., *Astronomy & Astrophysics*, 248, 281 (1991).
[7] Schmider, F.-X., Gay, J., Gaulme, P., et al, SYMPA, a dedicated instrument for Jovian seismology. I. Principle and performance, *Astronomy and Astrophysics*, Volume 474, Issue 3, pp.1073-1080 (2007).
[8] Soulat, L.; Schmider, F.-X., et al., Echoes: a new instrumental concept of Doppler Spectro-Imager for the ESA mission project JUICE, *Optical Complex Systems: OCS11*, Proceedings of the SPIE, Volume 8172 (2011).
[9] Wyant, J. C., Use of an ac heterodyne lateral shear interferometer with realtime wavefront correction systems, Applied Optics, 14, 2622–2626 (1975).